Available online at www.sciencedirect.com

jmr&t Journal of Materials Research and Technology

journal homepage: www.elsevier.com/locate/jmrt

Original Article

Reuse of iron ore tailings for production of metakaolin-based geopolymers

Igor Crego Ferreira [a,*], *Roberto Galéry* [a], *Andréia Bicalho Henriques* [a], *Ana Paula de Carvalho Teixeira* [b], *Caroline Duarte Prates* [b], *Athos Silva Lima* [b], *Isnaldi R. Souza Filho* [c]

[a] *Departamento de Engenharia de Minas, Universidade Federal de Minas Gerais, Belo Horizonte, MG, 31270-901, Brazil*

[b] *Departamento de Química – ICEX, Universidade Federal de Minas Gerais, Belo Horizonte, MG, 31270-901, Brazil*

[c] *Max-Planck-Institut für Eisenforschung Gmbh, Max-Planck-Straße 1, 40237 Düsseldorf, Germany*

ARTICLE INFO

Article history:
Received 31 January 2022
Accepted 31 March 2022
Available online 12 April 2022

Keywords:
Iron ore tailings
Metakaolin
Geopolymer
Alkaline activated material

ABSTRACT

Mining tailings are becoming more and more abundant and consequently it has been shown to be a material of great concern, especially after the dam failures in Brazil, Bento Rodrigues, 2015 and Brumadinho, 2019. In this work, iron ore tailings (IOT) were used as an aggregate in the production of geopolymers based on metakaolin used as a precursor and activated in alkaline solution. The alkaline solution was produced from a commercial solution of sodium silicate Na_2SiO_3 (SS) and a 10 M solution of sodium hydroxide NaOH (SH) prepared from solid flakes (3:1 mass ratio of SS:SH). Two syntheses were carried out, one by mixing metakaolin (MK) with the activator solution (AS) (1:1 mass ratio of MK:AS), called matrix, and another with the addition of aggregate (AG) to the matrix (1:1:2 mass ratio of MK:AS:AG), called geopolymer. XRD, FTIR, Mössbauer and SEM were used to analyze the inputs and materials produced, in addition to the analysis of compressive strength. The matrix reached a strength of 45.88 MPa with 7 days of curing, while the addition of IOT generated an increase in strength to the material, reaching values between 59.59 and 64.90 MPa also with 7 days of curing.

1. Introduction

Iron oxide concentrates usually composed by magnetite (Fe_3O_4) and hematite (Fe_2O_3), when submitted to metallurgical processes in presence of reductants, will produce metallic iron alloys. Despite 50 countries in world been responsible for producing all iron ore concentrates, Australia and Brazil dominate three quarters of total world production [17].

Most iron ore concentrate are exploited from low grade deposits. The growing iron ore demand have led to increase tailings production in the mineral processing plants [14]. Tailing dams consist of the mostly employed engineering structures built for high-capacity tailing storage [2]. The larger the tailings dam, the grater is the concern about its geotechnical stability and failure of these structures can lead to catastrophic consequences including human, environmental

* Corresponding author.
E-mail address: igorcrego@ufmg.br (I.C. Ferreira).

https://doi.org/10.1016/j.jmrt.2022.03.192

and economic loses [2,14]. The risk of tailings dams failure is a concern of the whole world since the recent tailing dams accidents, Brumadinho (Brazil), Bento Rodrigues (Brazil) Kayakari (Japan), Karamken (Russia) [13]. Most mineral industry plants are adapting to more sustainable tailing storage processes focusing on testing better tailings disposal methods including dry stacking and storage in exhausted pits [7,15]. Other tendency observed for new iron ore projects is the improvement of mining methods and plant designs obtaining dried and low-grade tailings with reduced masses and consequently, geotechnically more stable [9,16].

Co-products (geopolymers) can also be produced using tailing eliminating or reducing the storage in tailing dams [5,10]. Geopolymers are ceramic-like inorganic polymers produced at low temperature, usually below 100 °C, and consist of chains or networks of mineral molecules linked together by covalent bonds, in which the raw materials are mainly minerals of geological origin, hence the name "geopolymer" [4]. According to [10] alkali-activated materials (AAM) involve the synthesis reaction of raw materials rich in silicon and aluminum with a highly alkaline solution. When Al and Si ions are released into solution, they begin to form a new 3D network sharing oxygen atoms. Other elements, such as Fe, Mg and Ca, also contribute to this reaction, forming hydrated calcium (sodium) aluminosilicate (Ca-(N)-A-S-H) or double hydroxide with Mg-Al layer. When the calcium content is low, alkali-activated materials are called geopolymers, generating hydrated aluminosilicate (sodium) (N-A-S-H) [10]. However, NASH may not be a good abbreviation, as geopolymers after hardening form polymers with a stable three-dimensional network, having no water or hydroxyls in their structure [3].

The potential usage of mine tailings as a raw material with AAM has attracted many researchers and laboratory-scale studies have been conducted [5,10,11]. These applications are becoming a challenge due to the low reactivity of tailings, evidenced by their mineralogical composition. However, they can be used as an inert load in the AAM technology having as precursors materials, metakaolin, fly ash or blast furnace slag [10]. This recent technology can be used in several ways and for numerous productive purposes, such as encapsulation of waste (toxic or not), cements for concrete, geotechnical stabilizers for piles of waste and tailings and much more [1,3,10].

2. Materials and methods

2.1. Materials

The iron ore tailings (IOT) were obtained from Samarco's iron ore concentrator (Brazil). The metakaolin (MK) was obtained from Jundiaí, São Paulo, Brazil. The alkaline activator, the sodium hydroxide flakes, NaOH and sodium silicate Na_2SiO_3 were commercial products obtained with purity greater than 97%.

2.2. Alkali activator solution and sample preparation

The alkaline activator solution was produced by mixing a 10 molar NaOH solution with a sodium silicate, Na_2SiO_3, solution in a mass ratio of 1:3.

Matrix (M) and a geopolymer mortar were prepared. As presented in Fig. 1, mortars containing the matrix (M) composed by a mixture of metakaolin (precursor) and alkaline activator solution in same mass ratio proportion (1:1). Geopolymer mortar was also prepared mixing metakaolin (precursor), the alkaline activator and the IOT as aggregate. The proportions mass ratio of (1:1:2) respectively. These products were mounted in 6 rows containing 9 mortars each. The mortars were mounted a cylindrical PVC mold, measuring 3.4 cm in diameter and 6.8 cm in height. In Fig. 1, from left to right the second row is composed by Matrix (M) and the other rows are composed by geopolymer mortars (B, C, D, E and F).

2.3. Characterization

Uniaxial compression tests for mechanical resistance evaluation were carried out in an EMIC 100 tons total capacity hydraulic press. Each test was conducted using a 30-ton cell. Resistance tests were performed for 1, 3 and 7 curing days. For each day 3 mortars were tested. The X-ray diffractometry (XRD) spectra of pulverized samples (<150 μm) was generated acquired by on a Philips-PANalytical diffractometer model PW3710, using CuKa radiation and a graphite monochromator, range 3 – 90° 2θ, step 0,02° 2θ time per count 3sec. The FTIR technique used was the attenuated total reflection (ATR) with diffuse reflection (DRIFT) that permit to obtain spectra of specific groups of the solids in differential IR 7absorption in specific wavelengths (4000–400 cm^{-1}). The samples were finely pulverized (<5 μm) and mounted in a transparent KBr matrix. The FTIR spectrometer used was a Bruker, model Alpha. The MEV/EDS was carried out in a Zeiss-Merlin Microscope. The EDS was made with working distance of 10 mm and beam acceleration of 15 kV. The Mössbauer tests were performed in a LakeShore Vibrant Sample Magnetometer, model 7400 series.

Fig. 1 – Specimens produced (from left to right the rows was classified by B, M, C, D, E and F, being only M a matrix and the others geopolymer).

3. Results and discussion

3.1. Physical-chemical characteristics of geopolymers

The iron ore tailings presented 86.25% of silicon dioxide (SiO_2), 11.89% of ferrous oxides, 0.43% of aluminum oxide and 0.57% of calcium oxide and its particle size distribution is presented in Fig. 2.

Chemical analysis performed on the Metakaolin (MK) presented the following results: 55.5% SiO_2, 36.5% Al_2O_3, 2.0% Fe_2O_3, 1.0% TiO_2 and 1.5% K_2O. The sodium hydroxide purity is higher than 97%. Sodium silicate contains a mass ratio (SiO_2/Na_2O) equal to 2.20, containing 14.88% Na_2O and 32.73% SiO_2, with a percentage of total solids of 47.61%.

3.1.1. X-ray diffraction – XRD

To participate in geopolymerization reactions precursors must be submitted to mechanical or thermal activation to alter the crystalline phase to an amorphous one. To enhance reactivity the crystalline phases must be composed by silicon and aluminum [12]. The IOT would enter exclusive as aggregate since this material did not undergo any previous activation treatment and also due to absence of aluminum atoms. According to [12]; due to the high activation costs the best choice for tailings with low reactivity is their application as aggregates in geopolymers.

Figure 3 shows the presence of quartz in all diffractograms. In addition to quartz, the main peak of kaolinite also appears in the metakaolin sample, however this peak has a very low intensity, which indicates that the material had good calcination and practically all the kaolinite was calcined, on the other hand, it shows that the ore used in the calcination was not a pure kaolinite, since the quartz phase was found, which did not undergo amorphization after thermal treatment. The matrix DRX spectra is quite similar to the MK spectra. Quartz and very low intensities are presented for kaolinite probably due to the alkaline activation of Al and Si atoms associated to the MK amorphous phase. In the IOT spectrum, it was identified quartz, hematite and goethite phases. The same phases identified for the IOT was found in the geopolymer spectrum. These phases do not appear in the diffractogram of the matrix, meaning that the presence of the IOT provided those crystalline phases, with exception of quartz that appears in the matrix, but the phase has a great increase in intensity. It is evident that IOT acts only as an aggregate producing an IOT geopolymer.

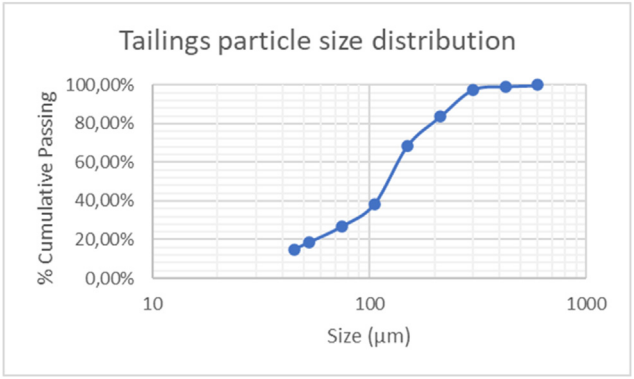

Fig. 2 – Tailings particle size distribution.

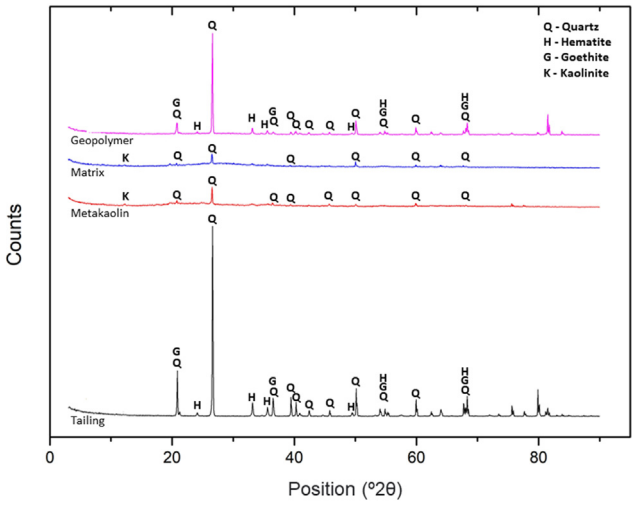

Fig. 3 – X-Ray Diffractometry of metakaolin and tailings inputs, and of matrix and geopolymer products.

3.1.2. Fourier transform infrared spectroscopy (FTIR)

The principal band characteristic of the amorphous $2SiO_2.Al_2O_3$ appears at approximately 1016–1037 cm^{-1} when standard metakaolin is under study [8]. According to [8]; the asymmetric stretching vibration band of Si–O–T (T = Si or Al) is responsible for this band and such values vary according to the increase in the content of the element T. The presence of Al-rich phases into the raw kaolin contributes to the shift of the band to lower wavelength values reaching 980 cm^{-1}. In turn, the wavelength increases for Si-rich phases reaching values above 1090 cm^{-1} [6] identified values around 1085 and 1057 cm^{-1} in wavelength of this band for IOT. In Fig. 4, this band can be identified in the metakaolin (1038 cm^{-1}), which indicates a kaolin not so rich in aluminum, but not with very high concentrations of Si, being a kaolin close to the standard. It was also possible to observe this

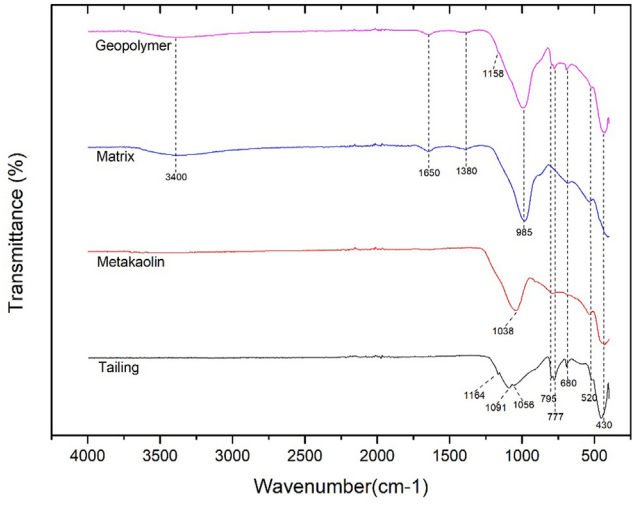

Fig. 4 – FTIR spectra of metakaolin and tailings inputs, and of matrix and geopolymer products.

band for the IOT, where the Al concentration is low and the Si concentration is very high, in which the values between 1056 and 1164 cm^{-1} are attributed to the asymmetric stretching vibration band of Si–O–T (T = Si-rich). A slight band is also observed in this interval in the geopolymer sample. During dissolution, the band changes slightly to low wavelength values: 1000 cm^{-1} and then 960–980 cm^{-1} when the geopolymerization process is completed, where the wavelength stabilizes around 987–1010 cm^{-1}, justifying the bands found around 985 cm^{-1} in the matrix and geopolymer spectra. The bands between 796 and 694 cm^{-1}, related to symmetrical vibrations of Si-O-T bonds [6], this band appears in the spectra of geopolymer, tailings and metakaolin. The stretching vibration band of the Fe-O bonds is centered at 518 cm^{-1} [6] and this appeared in every spectrum, attributed to the Fe bond. Stretching vibration bands are found between 3700 and 3600 cm^{-1} associated with O-H bonds and a small band at 1654 cm^{-1} is associated with the –OH bending vibration of water [6]. In the Figure above it can be seen clearly note the appearance of two regions of bands close to the values indicated in the geopolymer and in the matrix, which is possibly due to the residual water present in the bodies, however in the first case the bands are shifted to lower values. Another band that appears after the production at both mixes is the band at approximately 1380 cm^{-1}, which possibly indicates an excess of sodium in the chosen mixture, generating the production of sodium carbonate, since according to [8] the presence of bands between 1430 cm^{-1} and 1450 cm^{-1} is attributed to the asymmetric stretching of the O–C–O bonds in CO_3^{2-} formed by the reaction between the extra Na^+, K^+, … and atmospheric CO_2 on the surface of the geopolymer network [6]. identified the presence of sodium carbonate (Na_2CO_3) by the broad hump at approximately 2892 cm^{-1}, which was not observed in the matrix and geopolymer spectra, but due to its elongation, it may overlap with the stretching vibration bands of O-H bonds shifting it to lower wavelength values.

3.1.3. *Mössbauer*

The Mössbauer ^{57}Fe spectroscopy makes possible to differentiate Fe atoms combined with oxides from those associated with the geopolymers molecular structure in which Fe replaces Al [5].

The ^{57}Fe Mössbauer spectra allow to follow the transformation of ferro-kaolinite into ferro-metakaolin during calcination. Observing the two parameters of the doublet spectrum, IS (isomer-shift) and QS (quadrupole-Split), the value of QS increases considerably during calcination, from QS = 0.60 mm/s for initial ferro-kaolinite to QS = 1.00–1.50 mm/s at IS = 0,20. These final values are characteristic of Fe^{3+} atoms in the tetrahedral structural position [IV].

According to Fig. 5, the IS value obtained was 0.31 mm/s for metakaolin sample and 0.33 and 0.32 mm/s for the matrix samples. These values indicate the Fe^{3+} present in the kaolinite structure, however, as the quadrupole-Split QS values were 0.68 mm/s, 0.63 mm/s and 0.66 mm/s, respectively, not reaching higher QS values it is understood that the ferro-kaolinite structure present in metakaolin did not suffer changes to ferro-metakaolin. This means that the Fe atoms present in the structure of ferro-kaolinite do not convert into ferro-metakaolin and, consequently, are not substituting Al in

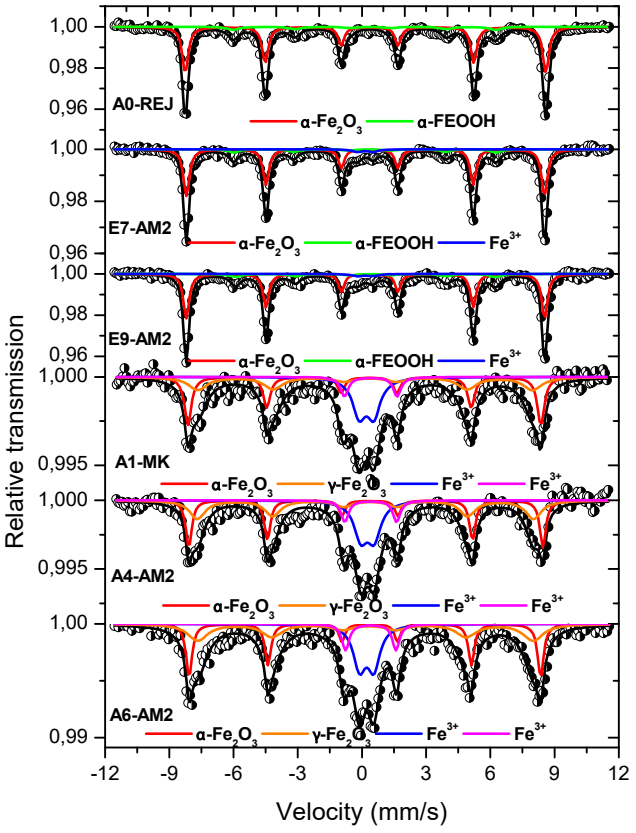

Fig. 5 – Mössbauer spectra of ^{57}Fe obtained at room temperature (RT) from the inputs metakaolin (A1-MK) and tailings (A0 – REJ), and from two samples of the matrix products (A4 and A6 - AM2) and geopolymer (E7 and E9 – AM2).

the geopolymer structure. The iron present in the IOT sample is found in the presence of oxides, since they all have the magnetic hyperfine splitting in their spectra. This is also evident from DRX and SEM tests results.

3.1.4. *Scanning electron microscopy (SEM)*

As can be seen in Fig. 6 of the SEM/EBSD, the Fe found in item F is present in specific locations that in the other items are dark, that is, they are not found in the presence of the other elements, with the exception of oxygen, again indicating that the Fe present in metakaolin is not acting in the geopolymer matrix as part of the tetrahedral network that gives rise to the structure of the material, but as a granular material in the aggregate function.

For the elements silicon and aluminum (items E and D, respectively) it is also possible to verify points of concentration of these elements, which probably represent quartz and kaolin particles, which did not undergo calcination or that the reaction with the activator did not take place. However, in some cases this reaction began to occur, as in those places in item C that are darker than the general matrix of the formed geopolymer bond, but which are not completely dark, as they are not free of sodium atoms. Completely dark places are those where the activator does not react.

It is possible to perceive a large geopolymer network, given that the elements O, Na, Si and Al appear forming a concise

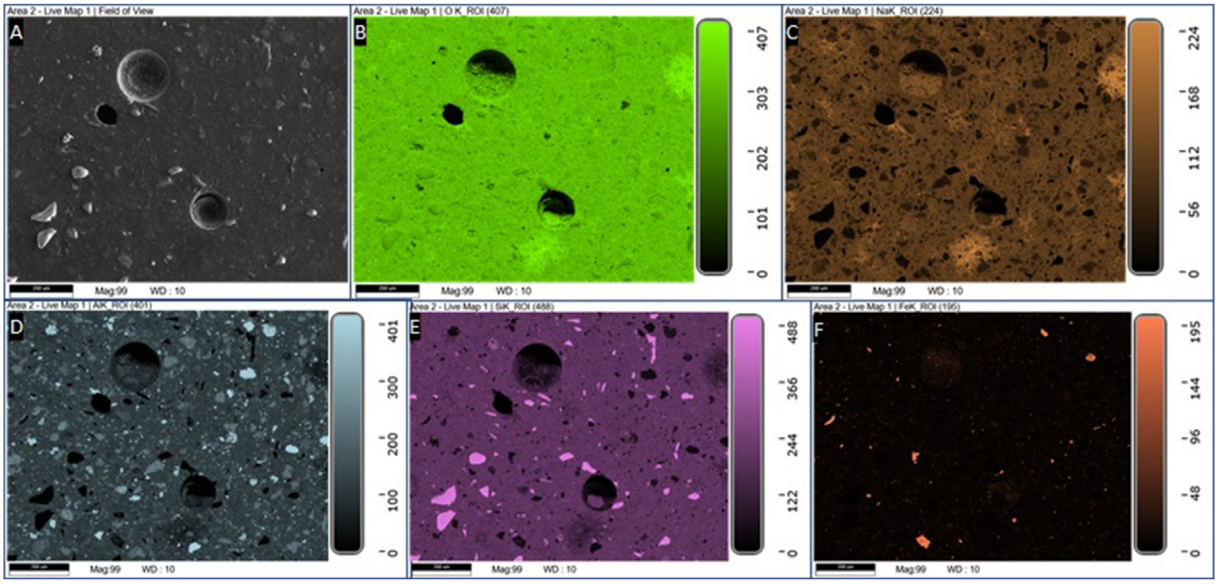

Fig. 6 – SEM of the matrix (A), with EBSD of the elements oxygen (B), sodium (C), aluminum (D), silicon (E) and iron (F).

structure in most of the sample, which indicates similar concentration of each element in the sample. These locations of continuous concentration of the elements indicate a well-formed network, indicating a very-well concentration of formed geopolymer.

3.2. *Compressive strength of geopolymers*

In Fig. 7, it can be verified initially that the increase in the strength gain of the geopolymer is greater in the first days, with around 50% of the gain in strength acquired on the seventh day being gained in the first 24 h for the geopolymers and around two thirds for the matrix. The compressive strength in the initial 24 h was awfully close for both materials. Then the increases were higher for the mortar (with IOT), and the material after 7 days of curing reached values between 59,59 and 64,90 MPa with geopolymers with tailings and 45,88 MPa for the material without aggregate.

This gain may be associated with some factors, such as the fact that the matrix is produced by mixing two parts, one solid and the other liquid, having a high water/total solids ratio (0,427:1), which is greatly reduced with the addition of aggregate (0,183:1) and, and that higher values of this relationship are considered a problem for cementitious materials in general, the rule being also valid for the case of geopolymers.

It is also understood that the water/alkaline ions ratio is not significantly altered only with the addition of water to improve workability, which would not generate problems in the dissolution of the inputs, however it is understood that with the addition of the aggregate, the attack of the ions to the precursor elements happens slowly, which can favor the construction of three-dimensional networks of geopolymers, creating more complex, bigger and more resistant structures.

The free water in the system could also generate an increase in matrix shrinkage, since the water would move more

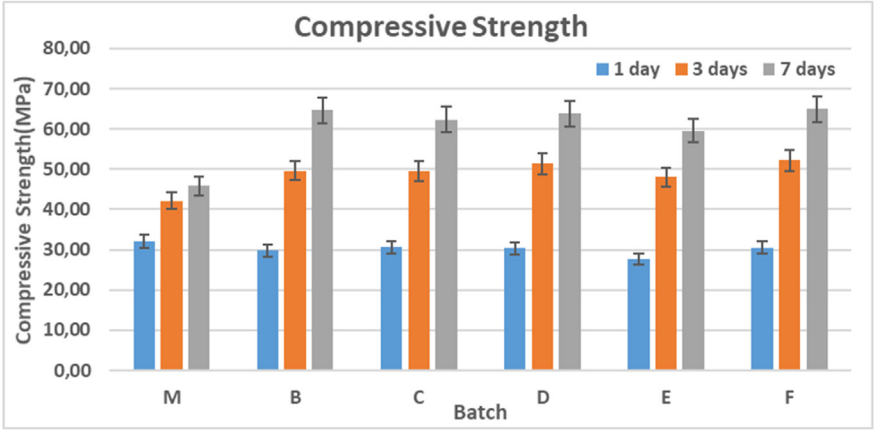

Fig. 7 – Compressive strength of matrix (M) and geopolymer mortar (B, C, D, E and F).

easily without the presence of the aggregate, so that it could be evaporated more quickly, and this, consequently, could generate a higher rate of cracks and structural problems. On the other hand, in the presence of aggregate, the curing would be slower, having water in the system for a longer period, helping in the greater formation of oligomers and generating larger chains of molecules that would withstand greater resistance, especially at higher curing times, As in the case of 7 days, where the strength gain in relation to strength on day 3 was close to 25% in specimens from C to F and 30% in specimens from B, while, in turn, the matrix specimens had a gain of less than 10% in their strength for the same period.

Another point of possible gain in the use of tailings is associated with the characterization generated by the effect that a filler material, that is, an aggregate of high fineness, as can be seen in Fig. 2, which can favor a mortar binding structure, increasing its workability, reducing its capillarity and the permeability of the mass produced, since the filler material acts with micro aggregates in the MAA, filling pore volume and making the microstructure denser.

4. Conclusions

Results from chemical and mineralogical characterization demonstrated that the metakaolin was not pure in composition presenting in its structure aluminosilicate particles that did not polycondense into geopolymer paste, which indicates that part of the kaolinite was not sufficiently calcined inducing problems dissolution. These aspects have a negative impact on the paste produced. However, in the broad sense it showed a good process of condensation in geopolymer as observed in SEM results and in the compressive strength, reaching 45.88 MPa in 7 days of curing.

The production of geopolymer mortar with IOT as aggregate increased the geopolymer compressive strength compared to the matrix one, however, this gain can be associated with some advantages when adding aggregates in cement pastes in the production of mortars and concretes. This was determined by the fact that IOT have a well-defined crystalline structure, as shown by the XRD results, and, even after the geopolymer polycondensation, the crystalline phases remained the same as analyzed previously.

The compressive strength result presented from both, matrix and mortars, were high indicating that these products can be used in some industrial applications. The geopolymers, produced with the addition of IOT as aggregate reached higher compressive strength than the matrix one, showing IOTs can act satisfactorily improving geopolymers quality.

The great compressive strength obtained with the IOT geopolymer compared to the matrix one can be explained by some factors, such as the high shrinkage in the matrix due to the easy movement of water in the paste without IOT, or the excess of water ratio to solid materials in the matrix. This is reduced in the IOT geopolymer since water is spelled way the IOT geopolymer structure.

It is also understood that the addition of aggregates has a maximum limit to increase the strength of the geopolymer, since low amounts of geopolymer matrix would result in little geopolymeric binding with no adhesion matrix/aggregate particles.

Declaration of Competing Interest

The authors declare that they have no known competing financial interests or personal relationships that could have appeared to influence the work reported in this paper.

Acknowledgment

The financial support from Brazilian research agencies Conselho Nacional de Desenvolvimento Científico e Tecnológico (CNPq), Coordenação de Aperfeiçoamento de Pessoal de Nível Superior – Programa de Excelência Acadêmica (CAPES-PROEX), and Fundação de Amparo à Pesquisa do Estado de Minas Gerais (FAPEMIG) is appreciated.

IRSF acknowledges financial support through CAPES (Coordenação de Aperfeiçoamento de Pessoal de Nível Superior) & Alexander von Humboldt Foundation (grant number 88881.512949/2020-01).

REFERENCES

[1] Assi LN, Carter K, Deaver E, Ziehl P. Review of availability of source materials for geopolymer/sustainable concrete. J Clean Prod 2020;263. Elsevier BV. https://doi.org/10.1016/j.jclepro.2020.121477.

[2] Carmignano OR, Vieira SS, Teixeira APC, Lameiras FS, Brandão PRG, Lago RM. Iron ore tailings: characterization and applications. J Braz Chem Soc 2021:1895–911. Sociedade Brasileira de Quimica (SBQ). https://doi.org/10.21577/0103-5053.20210100.

[3] Davidovits J. Geopolymer: chemistry and applications. 5th ed. Saint-Quentin: Institut Géopolymère; 2020a.

[4] Davidovits J. Review. Geopolymers: ceramic-like inorganic polymers. J Ceram Sci Technol 2017;8(3):335–50. Göller Verlag. https://doi.org/10.4416/JCST2017-00038.

[5] Davidovits J, Davidovits R. Ferro-sialate geopolymers. Technical papers # 27. Geopolymer Institute Library; 2020b. https://doi.org/10.13140/RG.2.2.25792.89608/2. www.geopolymer.org.

[6] Figueiredo RAM, Brandão PRG, Soutsos MHB, Fourie A, Mazzinghy DB. Producing sodium silicate powder from iron ore tailings for use as an activator in one-part geopolymer binders. Mater Lett 2021;288:129333. Elsevier BV. https://doi.org/10.1016/j.matlet.2021.129333.

[7] Fonseca H, das G de Á, Alexandrino JS, Ferreira TED. Metodologias de Disposição de Rejeitos de Minério de Ferro para Substituir as Barragens de Rejeito. Profiscientia 2019;12:54–72.

[8] Kamseu E, Alzari V, Nuvoli D, Sanna D, Lancellotti I, Mariani A, et al. Dependence of the geopolymerization process and end-products to the nature of solid precursors: challenge of the sustainability. J Clean Prod 2021;278:123587. Elsevier BV. https://doi.org/10.1016/j.jclepro.2020.123587.

[9] Kinnunen P, Obenaus-Emler R, Raatikainen J, Guignot S, Guimera J, Ciroth A, et al. Review of closed water loops with ore sorting and tailings valorisation for a more sustainable mining industry. J Clean Prod 2021;278. Elsevier BV. https://doi.org/10.1016/j.jclepro.2020.123237.

[10] Kiventerä J, Perumal P, Yliniemi J, Illikainen M. Mine tailings as a raw material in alkali activation: a review. Int J Miner Metall Mater 2020;27(8):1009–20. Springer Science and

Business Media LLC. https://doi.org/10.1007/s12613-020-2129-6.

[11] Perumal P, Piekkari K, Sreenivasan H, Kinnunen P, Illikainen M. One-part geopolymers from mining residues – effect of thermal treatment on three different tailings. Miner Eng 2019;144:106026. Elsevier BV. https://doi.org/10.1016/j.mineng.2019.106026.

[12] Ren B, Zhao Y, Bai H, Kang S, Zhang T, Song S. Eco-friendly geopolymer prepared from solid wastes: a critical review. Chemosphere 2021;267. Elsevier BV. https://doi.org/10.1016/j.chemosphere.2020.128900.

[13] Santos T,B, Oliveira RM. Failure risk of brazilian tailing dams: a data mining approach. Eng Sci 2021;93(4). https://doi.org/10.1590/0001-3765202120201242.

[14] Souza A H de, Von Krüger FL, Araújo FG da S, Mendes JJ. Mineralogical characterization applied to iron ore tailings from the desliming stage with emphasis on quantitative electron microscopy (qem). Mater Res 2021;24(3). FapUNIFESP (SciELO). https://doi.org/10.1590/1980-5373-mr-2019-0677.

[15] Stela LHP, Duarte JC, Pereira CO. Métodos de Disposição dos rejeitos de Minério de Ferro alternativos ao método de Barragens: uma revisão. Rev Brasil Process Químicos Camp, SP 2020;1(1):1–58.

[16] Suppes R, Heuss-Aßbichler S. Resource potential of mine wastes: a conventional and sustainable perspective on a case study tailings mining project. J Clean Prod 2021;297:126446. Elsevier BV. https://doi.org/10.1016/j.jclepro.2021.126446.

[17] USGS. Iron ore statistics and information. 2021. https://www.usgs.gov/.